

Active Vibration Suppression of a Flexible Blade Element Using Magnetorheological Layer Patch-Electromagnetic Actuator

Fevzi Çakmak Bolat^{1*} and Selim Sivrioğlu²

¹ Department of Mechanical Engineering, Bayburt University, 69000, Bayburt, Turkey

² Department of Mechanical Engineering, Gebze Technical University, 41400, Gebze, Turkey

Received: 10 October 2017; Revised: 27 December 2017; Accepted: 2 January 2018; Published: 1 June 2018

Turk J Electrom Energ Vol.: 3 No: 1 Page: 3-11 (2018)

SLOI: <http://www.sloi.org/>

*Correspondence E-mail: fevzibolat@bayburt.edu.tr

ABSTRACT This study proposes a new active control structure to suppress vibrations of a small-scale wind turbine blade with magnetorheological fluid (MR) patch actuated by an electromagnet. An interaction model of the MR patch electromagnetic actuator was derived and a force characterization was realized. A linear quadratic gaussian (LQG) controller was designed using the state space model of the flexible blade element. The LQG controller was experimentally realized by means of the blade structure under the impact load and steady state aerodynamic load conditions. The results of experiments showed that the MR patch is effective for suppressing vibrations of the blade structure.

Keywords: Active Vibration Control, MR Patch Actuator, LQG Control, Flexible Blade

Cite this article: F. C. Bolat, S. Sivrioğlu, Active Vibration Suppression of a Flexible Blade Element Using MR Layer Patch-Electromagnetic Actuator, *Turkish Journal of Electromechanics & Energy* 3(1) 3-11 (2018)

1. INTRODUCTION

Active vibration control system improves the performance of the structures in terms of reduction in vibration amplitude compared to passive systems. Actively controlled flexible structures with embedded piezoelectric (PZT) layers have been studied by many researchers to create smart or adaptive structures for responding on changing external conditions. Although PZT layer has great potentials especially for aerospace applications, there are some difficulties in its realization for large engineering systems.

The magnetorheological fluids are non-Newtonian fluids consisting of ferromagnetic particles that can change its rheological properties under application of an external magnetic field. The MR fluid has distinct properties for engineering applications and can be used in vibration control studies [1-4]. One of the most known engineering applications of the MR fluid is the MR damper used in vehicle suspensions with semi-active control. In these dampers, the damping force is controlled by changing the viscosity of the MR fluid with applied electric current of a coil inside the damper. The MR fluid was also used in the active vibration control of structural systems [5-6]. Many researchers

examined the behavior of sandwich structures containing MR fluid under a magnetic field and active vibration control [7-9]. Valevate studied the analytical modeling and the potential use of MR fluids for performing semi-active vibration control [10]. Rajamohan et al proposed a semi-active control synthesis which was presented to control the dynamic characteristics of fully and partially treated MR sandwich beams [11]. The governing equations for the motion of a three-layer MR sandwich beam were expressed in the state variable form, and an observer-based linear quadratic regulator (LQR) optimal control strategy was developed. Hirunyapruk performed an adaptive tuned vibration absorber (ATVA) exploiting the changeable properties of MR fluids in the pre-yield state [12]. This ATVA has been experimentally worked with PID control.

In this study, the ferromagnetic feature of the MR fluid is employed for an electromagnet actuator. The MR layer patch is attached on a flexible blade element and attracted by the electromagnet to suppress the vibration of the flexible structure. In this case, the force is generated by the magnetic field of the electromagnet and there is no contact during operation. It is also

^cInitial version of this paper was selected from the proceedings of International Conference on Advanced Engineering Technologies (ICADET 2017) which was held in September 21-23, 2017, in Bayburt, TURKEY; and was subjected to peer-review process prior to its publication.

possible to use an iron plate as an attracting element for the electromagnet instead of using MR layer patch. Nevertheless, the iron plate in the same volume of the patch is 2.5 times heavier than the MR patch and this may change the natural frequencies of the attached structure. In addition, homogeneity and rigidity of the structure may be deteriorated if a ferromagnetic metal fixed on the flexible structure. Moreover, the MR layer patch is easily formed and may take the shape of the structure when it is attached.

Active vibration control of wind turbine wings is an important research topic and was studied in reference [13]. To implement the proposed MR patch electromagnetic actuator, a small-scale wind turbine blade is selected to suppress modes of vibration. In a wind turbine, when the air flows over the turbine blades with a certain angle of attack, lift and drag forces occur and drag forces cause vibrations on the blade. To reflect the real system disturbances in the experimental system of this study, an aerodynamic load was generated, and the designed controller was tested under such effects.

2. MODELING OF THE BLADE STRUCTURE

The blade structure is produced based on the airfoil with code number SH3055 and characteristics and wind tunnel aerodynamic tests for this airfoil are reported in reference [14]. The airfoil is designed for use on small wind turbines. The blade structure is manufactured by a small wind turbine manufacturer [BRZ Enerji, Istanbul, TR] with an aluminum extrusion machine. The airfoil is made hollow to reduce the weight of the blade as shown in Figure 1(b).

2.1 State-Space Model

The layout of the cantilever blade structure with MR patch layer for control design study is shown in Figure 1(a). Here, x coordinate is related with the longitudinal dynamics and w coordinate shows the direction of vibration of the blade. The force that MR patch generated is shown by f and applied to the beam at the distance x_a . Also, f_d shows the disturbance force applied at the distance x_d . The distance x_s denotes the sensor location. The airfoil of the blade is shown in Figure 1(b). An inertia equivalent rectangular shape is calculated for modeling purposes.

For each vibration mode of the cantilever blade structure, the separated equation of motion is given in Eq.1 [16].

$$\ddot{x}_n(t) + 2\zeta\omega_n\dot{x}_n(t) + \omega_n^2x_n(t) = f(t)\psi_n(x_a) + f_d(t)\psi_n(x_d) \quad (1)$$

Where ω_n is the mode natural frequency, ζ is the damping coefficient and $\psi_n(\cdot)$ is the mode shape function. The state space equation for each modal behavior is obtained using Equation (1) as follows;

$$\dot{\bar{x}}_n(t) = A_n\bar{x}_n(t) + B_nu(t) + D_{wn}d(t) \quad (2)$$

where $\bar{x}_n(t)$ is the state vector, A_n is the system matrix, B_n is the control input matrix, and $u(t)$ is the control input. The structure of the state vector and matrices are as follows;

$$\bar{x}_n = \begin{bmatrix} x_n(t) \\ \dot{x}_n(t) \end{bmatrix}, A_n = \begin{bmatrix} 0 & 1 \\ -\omega_n^2 & -2\zeta\omega_n \end{bmatrix}, \quad (3)$$

$$B_n = \begin{bmatrix} 0 \\ \psi_n(x_a) \end{bmatrix}, D_{wn} = \begin{bmatrix} 0 \\ \psi_n(x_d) \end{bmatrix}$$

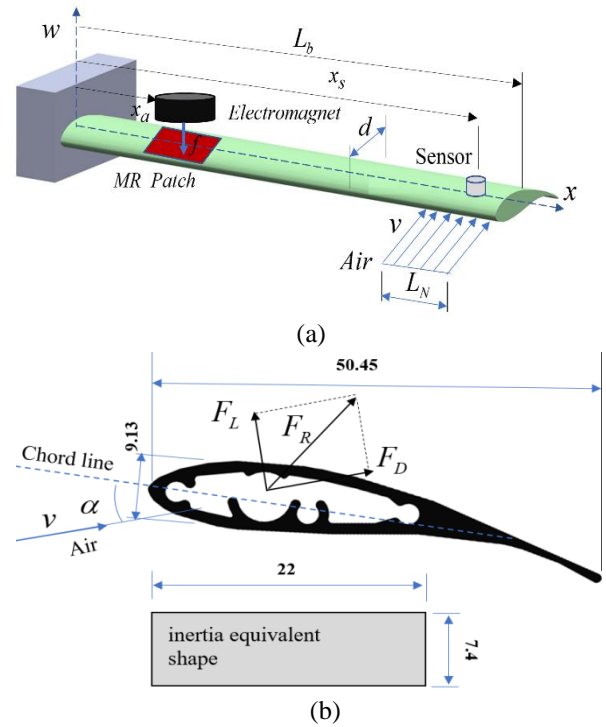


Fig. 1. Control system structure; (a) layout of the cantilever blade, (b) airfoil and its inertia equivalent rectangular shape

In distributed parameter systems, the displacement measured by the sensor is modeled as the multiplication of the modal displacement with the mode shape function at the considered point. For the sensor location, the modal output is written as;

$$w(x,t) = \sum_{i=1}^{\infty} x_n(t)\psi_n(x_s) \quad (4)$$

Using Equation (4) the output of the state space equation is obtained for each vibration mode as;

$$y_n = C \bar{x}_n(t) = [C_n \quad 0] \bar{x}_n(t) \quad (5)$$

where the matrix C_n is computed using the following mode shape function.

$$C_n = \psi_n(x_s) = \sinh \beta_n x_s - \sin \beta_n x_s - \left[\frac{\sinh \beta_n L_b + \sin \beta_n L_b}{\cosh \beta_n L_b + \cos \beta_n L_b} \right] (\cosh \beta_n x_s - \cos \beta_n x_s) \quad (6)$$

Where;

$$\beta_n = \left(\omega_n \sqrt{\frac{\rho A}{EI}} \right)^{1/2} = \left(\frac{2n-1}{2} \pi + e_n \right) \frac{1}{L} \quad (7)$$

If the modeling is extended for N modes ($n=1, \dots, N$), the state space structure is obtained as follows;

$$\dot{x}_f = \begin{bmatrix} \dot{\bar{x}}_1 \\ \dot{\bar{x}}_2 \\ \vdots \\ \dot{\bar{x}}_N \end{bmatrix} = \begin{bmatrix} A_1 & & & 0 \\ & A_2 & & \\ & & \ddots & \\ 0 & & & A_N \end{bmatrix} \begin{bmatrix} \bar{x}_1 \\ \bar{x}_2 \\ \vdots \\ \bar{x}_N \end{bmatrix} + \begin{bmatrix} B_1 \\ B_2 \\ \vdots \\ B_N \end{bmatrix} u + \begin{bmatrix} D_{w1} \\ D_{w2} \\ \vdots \\ D_{wN} \end{bmatrix} d \quad (8)$$

$$y_f = [C_1 \ C_2 \ \dots \ C_N] \begin{bmatrix} \bar{x}_1 \\ \bar{x}_2 \\ \vdots \\ \bar{x}_N \end{bmatrix}$$

A reduced order state space model for the control design study can be obtained by considering the first two modes of Equation (8). The reduced order state space equation is written as;

$$\begin{aligned} \dot{x}_r(t) &= A_r x_r(t) + B_r u(t) + D_{wr} d(t) \\ y_r(t) &= C_r x_r(t) \end{aligned} \quad (9)$$

Distributed parameter systems have theoretically infinite number of vibration modes. The state space model obtained as a full model in equation (8) considers certain number of modes. In this study, the full order model of the cantilever blade is built by considering the vibration modes up to 1.25 kHz. In practice, the modal contributions of the higher order modes are inconsiderable due to small modal amplitudes. Also, the reduced order model which contains the first two modes up to 60 Hz is used for controller designs. The frequency responses of the full and reduced order models are shown in Figure 2.

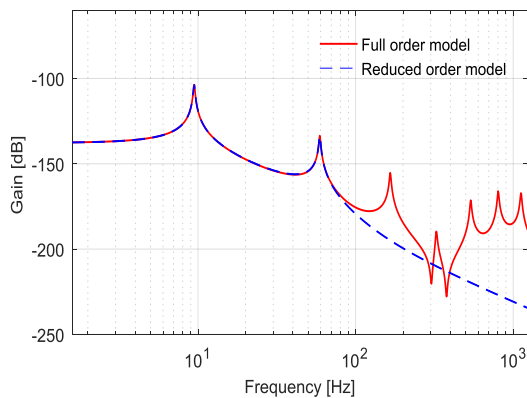


Fig. 2. Frequency response of the blade model

2.2 MR Patch and Actuator System

The MR fluid is filled into the locked plastic bag and glued to ensure that leak-proof as shown in Figure 3. The MR patch stick on the blade with a tape was used to prevent bag flexibility under magnetic field.

The thin plastic bag filled with MR fluid is fixed on the blade element as shown in Figure 4(a). The electromagnet is positioned opposing the MR patch with an air gap over the blade element to apply magnetic field to the MR patch as illustrated in Figure 4(b). When the current is applied to the electromagnet, a magnetic field is created, the iron particles in the MR patch become ordered and an attractive force on the blade is generated so that the vibrations are suppressed. The magnitude of the force depends on the magnetic flux given by the controller based on the displacement information of the blade obtained using an optical sensor in a feedback control structure.

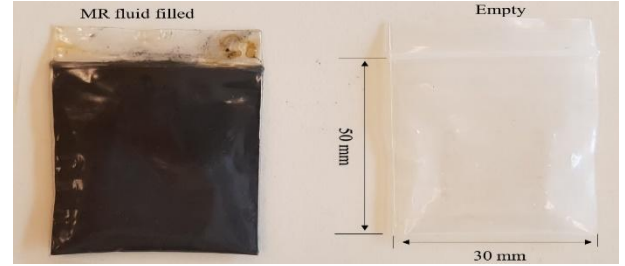
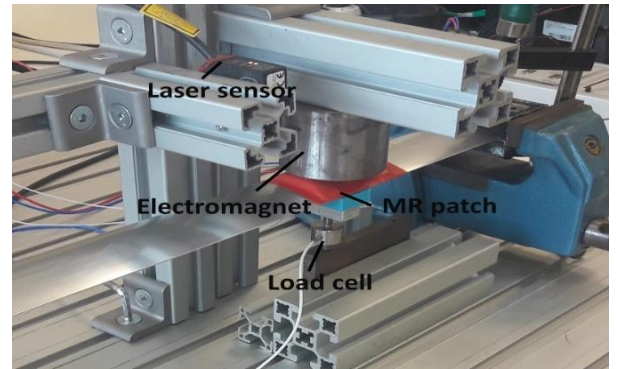


Fig. 3. Structure of the MR fluid patch



(a)



(b)

Fig. 4. (a) Electromagnet and MR patch in the experimental setup, (b) MR patch attached on the blade

2.3 Force Characterization

The interaction between the electromagnet and the MR patch is illustrated as a cross-sectional view in Figure 5. At the initial state as shown in Figure 5(a), the electromagnet is positioned over the blade with an air gap of w_0 . When the current is applied to the electromagnet in Figure 5(b), the MR patch is attracted by the electromagnet and an extension of ε is occurred due to flexibility of the plastic bag. At this stage, the blade does not move and the magnetic force and current that extend the MR patch are f_0 and i_0 , respectively.

After the extension of the patch is over the MR patch with the blade move toward the electromagnet. The electromagnetic force is defined as;

$$f(t) = k \frac{(i_0 + i_c(t))^2}{[w_0 - (\varepsilon + w(t))]^2} \quad (10)$$

where $k = 1/4\mu_0 N^2 A$. Here, A is the area of the electromagnet, N is the number of the coil turn and μ_0 is the vacuum permeability. Also, i_c is the control current. The electromagnetic force is linearized around (i_0, w_0) values as follows. The system parameters are given in Table 1.

$$f(t) = K_w w + K_i i_c \quad (11)$$

$$K_w = 2k \frac{i_0^2}{w_0^3}, \quad K_i = 2k \frac{i_0}{w_0^2}$$

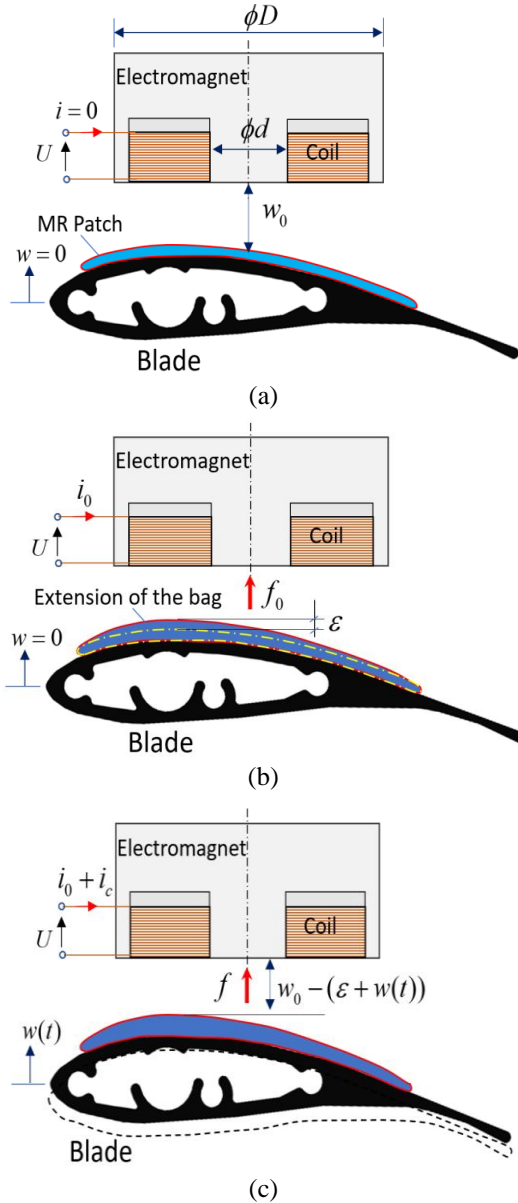


Fig. 5. Interaction model between the electromagnet and the MR patch; (a) initial state (b), extension of MR patch, (c) control of the blade

Table. 1 Values of the blade system parameters

Symbol	Meaning	Value	Unit
L_b	Length of the blade	800	mm
x_a	Distance of the actuator	150	mm
x_s	Distance of the sensor	700	mm
N	Number of the coil turn	221	-
A	Area of the electromagnet	2e-4	mm ²
μ_0	Vacuum permeability	12.5e-6	-
d	Width of the blade	50	mm

Since the MR patch has elasticity at certain extent, the response force of the MR patch layer to the electromagnet force input should be investigated. It is important to show how much electromagnetic force is transmitted to the MR patch. To understand the force variation at the MR patch side a load cell is installed under the blade as shown in Figure 4(a). It is not possible to measure electromagnetic force directly, but the magnetic field can be measured by a gauss meter. The experimental force f_e exerted by the electromagnet obtained using the experimental data with the following equation;

$$f_e = \frac{A}{\mu_0} B^2 \quad (12)$$

where B is magnetic field measured by using a Gaussmeter. The variations of the experimental forces are shown in Figure 6. In these experiments, the air gap between the electromagnet and MR patch is set to 1 mm. Table 2 also shows the data of the measured experimental forces in different currents. At large coil currents, the loss is increasing as seen in Table 2 and Figure 6.

Table 2. The measured forces in different current

Applied Current (A)	Force at MR Patch side (N) (Measured with load cell)	Electromagnet Force (N) (Measured with Gaussmeter)	Loss %
5	13.87	16.77	17.29
4.5	11.76	13.93	15.57
4	9.88	11.30	12.56
3.5	8.02	8.92	10.08
3	6.10	6.61	7.71
2.5	4.21	4.58	8.07
2	2.56	2.92	12.32
1.5	1.51	1.62	6.79
1	0.63	0.74	14.86
0.5	0.16	0.18	11.11

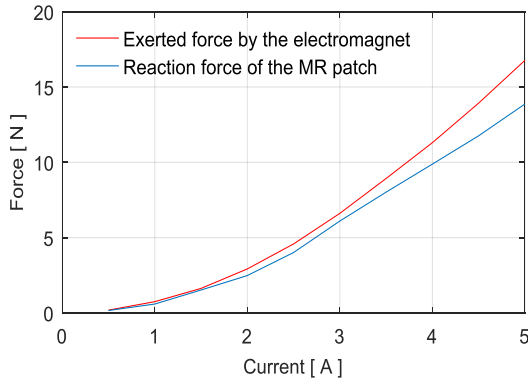


Fig. 6. Variation of the experimental electromagnetic force and response force exerted by MR patch

2.4 Aerodynamic Load

To test the designed LQG controller under a steady state disturbance, an aerodynamic load effecting on the blade structure is created using an air nozzle. In the case of wind turbines, the air current flows over the wings with a certain angle of attack. Lift and drag forces occur as the air passes over the blades and drag force causes vibrations on the blade. The forces are defined as;

$$F_L = \frac{1}{2} C_L \rho L_N d_b v^2 \quad , \quad F_D = \frac{1}{2} C_D \rho L_N d_b v^2 \quad (13)$$

where C_L and C_D are lift and drag coefficients. Also, L_N is the air load length, d_b is the width of the blade and v is the relative wind speed. The wing is forced to bend the blade by the effect of aerodynamic drag force F_D . The lift and drag coefficient data of the SH3055 airfoil used in the blade element of this study is given in reference [15]. Using these data, the variation of C_L and C_D with angle of attack is shown in Figure 7.

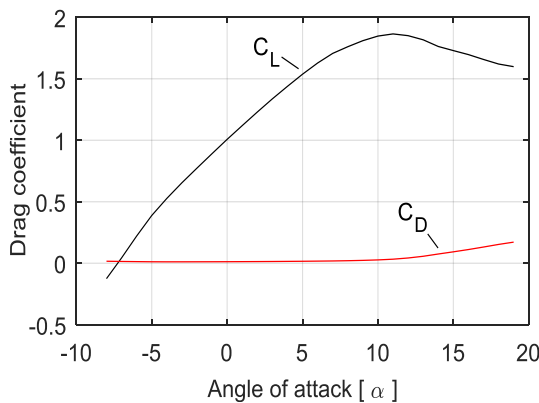
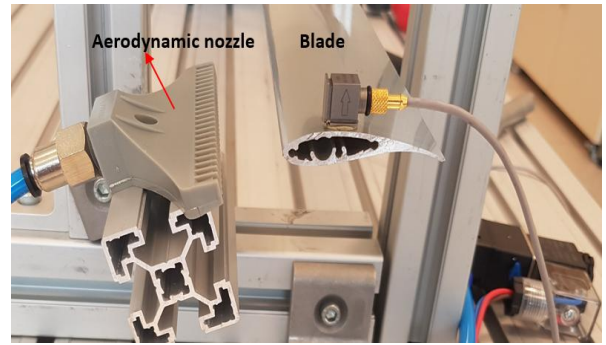
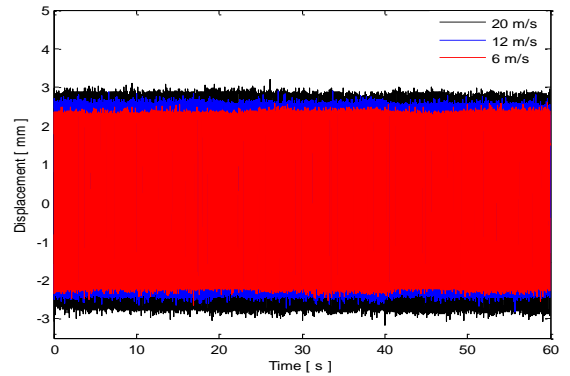


Fig. 7. Aerodynamic load characteristics lift and drag coefficients



(a)



(b)

Fig. 8. (a) Air nozzle effecting aerodynamic load on the blade element, (b) Steady state vibration of the blade element at different wind speeds

An air nozzle is used to create the aerodynamic load in the experimental setup of the blade structure as illustrated in Figure 8(a). Air nozzle blows air to the end of the blade element in adjusted air speeds. In the experimental system, it is observed that the blade starts to vibrate at the angle attack of 14° of the nozzle due to increasing of the drag force on the blade. In this study, the angle of attack of the air nozzle is set to 17.2° . The steady state vibration of the blade element at different wind speeds is illustrated in Figure 8(b).

3. LQG CONTROL DESIGN

LQG control is a modern control design method and it is a combination of the optimal control (LQR) with the optimal state estimation (Kalman filter). The active vibration control system in a feedback structure is shown in Figure 9.

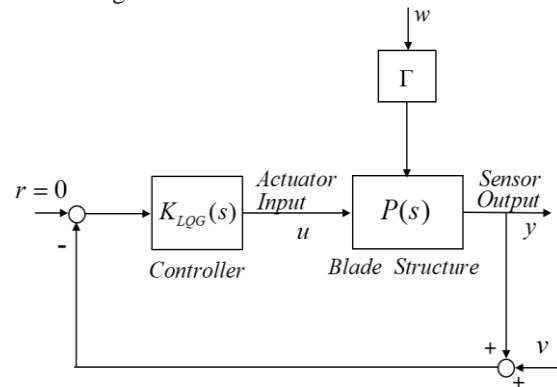


Fig. 9. Feedback control system structure

In general, LQG control improves the time domain responses of the structural vibration systems. The state space model obtained in Equation 11 for the blade element is considered as LQG control design model as follows;

$$\begin{aligned} \dot{x}_r(t) &= A_r x_r(t) + B_r u(t) + D_{wr} d(t) + \Gamma w(t) \\ y_r(t) &= C_r x_r(t) + v(t) \end{aligned} \quad (14)$$

where $w(t)$ is the system noise and $v(t)$ is the observation noise. These are zero mean, white, uncorrelated Gaussian random signals. The LQG control problem aims to minimize the cost function.

$$J = \lim_{t_f \rightarrow \infty} \frac{1}{t_f} E \left[\int_0^{t_f} [x^T(t) Q x(t) + u^T(t) R u(t)] dt \right] \quad (15)$$

Where $E\{\cdot\}$ is the statistical expectation operator. Also, Q and R are the weighting matrices applied to the states and control inputs, respectively. The state estimate \hat{x}_r is formed using the Kalman filter state estimator as follows;

$$\dot{\hat{x}}_r(t) = A_r \hat{x}_r(t) + B_r u(t) + K_f (y_r(t) - C_r \hat{x}_r(t)) \quad (16)$$

where K_f is the Kalman filter gain and computed as;

$$K_f = S C_r^T V^{-1} \quad (17)$$

Here S is the solution of the Algebraic Riccati Equation.

$$A_r S + S A_r^T - S C_r^T V^{-1} C_r S + \Gamma W \Gamma^T = 0 \quad (18)$$

Where V and W are the spectrum of the system and observation noises. The optimal control is formed using the LQR state feedback gain matrix F and the estimated state \hat{x}_r .

$$u(t) = -F \hat{x}_r \quad (19)$$

It is possible to combine the optimal control and Kalman filter by substituting Equation (19) into (16) and arranging in the state space form.

$$\begin{bmatrix} \dot{\hat{x}}_r \\ u \end{bmatrix} = \begin{bmatrix} A_r - B_r F - K_f C_r & K_f \\ -F & 0 \end{bmatrix} \begin{bmatrix} \hat{x}_r \\ y_r \end{bmatrix} \quad (20)$$

The LQG controller is in the state space form with the following controller matrices.

$$K_{LQG} = \begin{bmatrix} A_r - B_r F - K_f C_r & K_f \\ -F & 0 \end{bmatrix} = \begin{bmatrix} A_k & B_k \\ C_k & D_k \end{bmatrix} \quad (21)$$

The LQG control block structure is shown in Figure 10. The frequency response characteristics of the LQG controller is depicted in Figure 11. The closed-loop frequency response of the system is presented in Figure 12. The LQG controller suppressed the targeted vibration modes with significant reduction in magnitudes of the blade system.

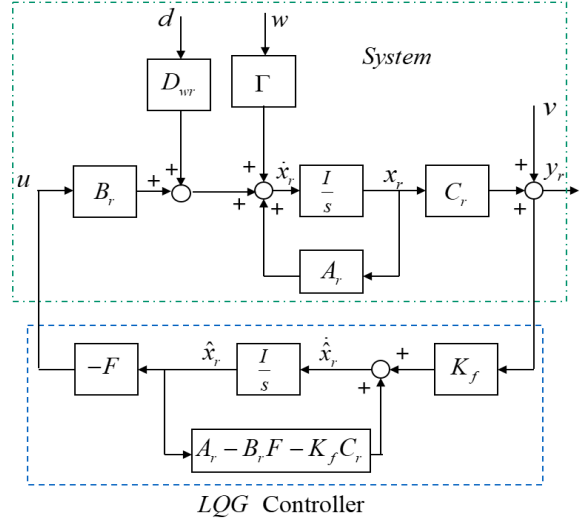


Fig. 10. LQG control structure

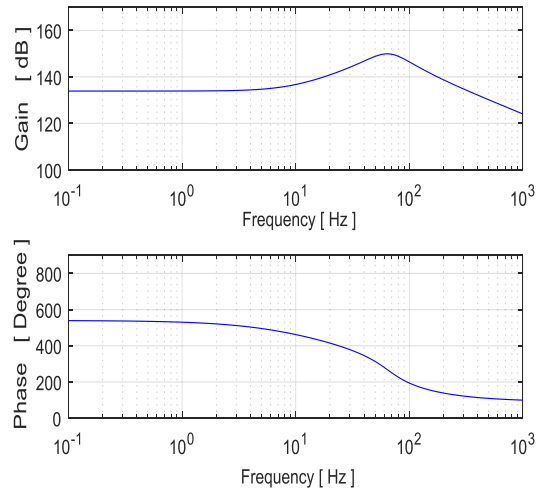


Fig. 11. Frequency responses of the LQG controller

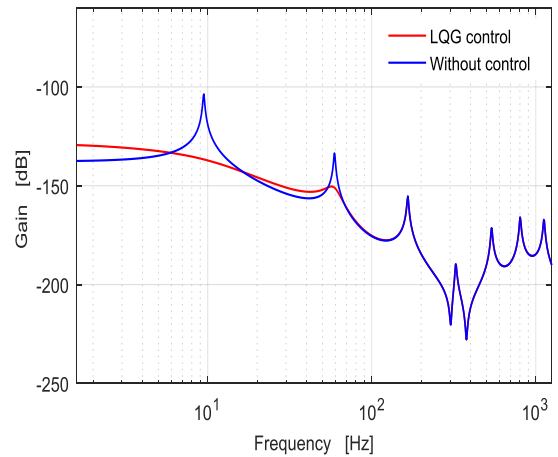


Fig. 12. Frequency responses of the closed loop system

4. EXPERIMENTAL SYSTEM

The photo of the experimental system setup is shown in Figure 13. An aluminum alloy 6060 elastic blade which is used in a small-scale wind turbine test system is studied for vibration suppression purposes. A MR patch is attached on the surface of the blade and the blade is fixed at one end using a clamp. In the experimental system, a current drive is used to drive the electromagnet. Vibration analysis of the blade is performed with a Bruel&Kjaer 3053 device. The designed LQG controller is realized using dSpace 1104 control card. The controller is discretized and compiled in the state space form using a Matlab/Simulink file and installed on dSpace control card.

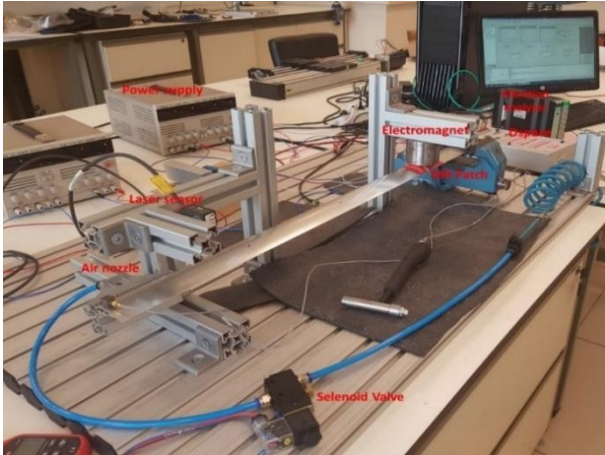


Fig. 13. Experimental system setup

The experimental frequency responses of the closed loop system with the LQG controller is obtained and presented in Figure 14(a). The results of the first two modes for the control design is also shown in Figure 14(b).

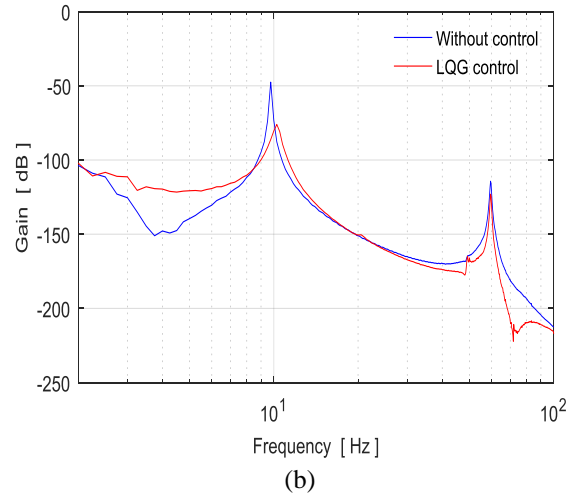
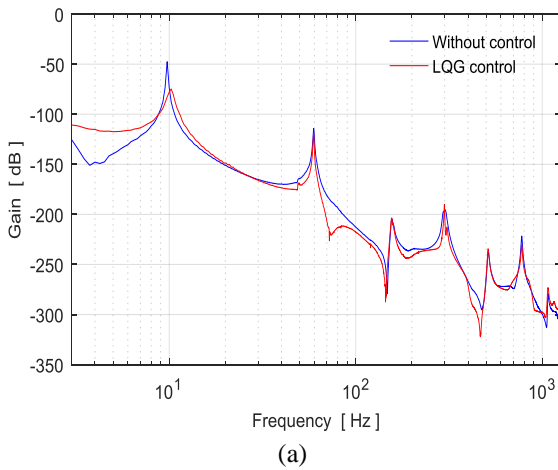
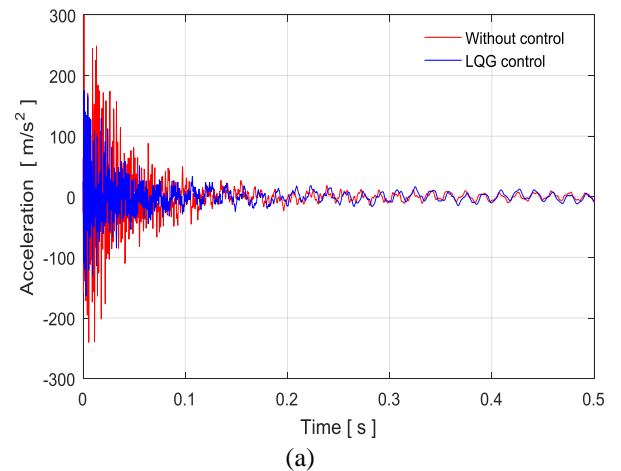


Fig. 14. Experimental frequency responses of the closed loop system; (a) full system, (b) first two modes

Table 3. Amount of reduction in gains with LQG control

Mode Number	Gain reduction [dB]
1 st mode	28.55
2 nd mode	8.7

The amount of reduction in the closed loop frequency response gain is summarized in Table 3. The LQG controller provided significant gain reduction in the first vibration mode of the blade element. The reduction in the second mode is also at acceptable level. Since an ideal mathematical model is used in the simulation, the frequency response of the closed loop in the simulation shows a smooth significant reduction in gains. In real systems, there are some unmodeled dynamics and the experimental results demonstrate some differences with simulation results. On the other hand, the overall trend in the closed loop frequency responses of the simulation (Figure 12) and experimental (Figure 14) results are in accordance with each other.



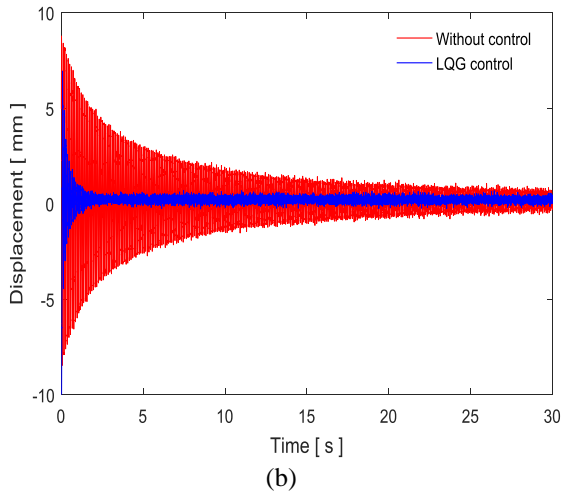


Fig. 15. Experimental time history responses of the closed loop system; (a) acceleration, (b) displacement

At first a transient response analysis is realized with LQG controller. The transient time history responses of the closed loop system with LQG control are shown in Figure 15.

The control effectiveness is good at acceleration and displacement responses. When the air nozzle blows air to the end of the blade element in adjusted air speeds, the blade element starts to vibrate due to drag forces on it. This creates a steady state aerodynamic load on the blade. Note that air speed is taken as 15 m/s in the experiments. The designed LQG controller is tested under the steady state aerodynamic load. Experimental time history responses of the closed loop system for a continuous control case from a starting time are shown in Figure 16. Moreover, the repeated controlled and uncontrolled tests are realized to understand the response characteristics of the controller as given in Figure 17. The controller shows the better control effectiveness to attenuate vibrations of the blade.

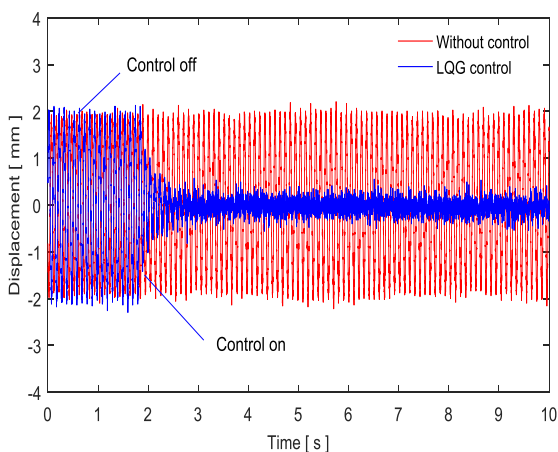


Fig. 16. Experimental results of the closed loop system with steady state aerodynamic load

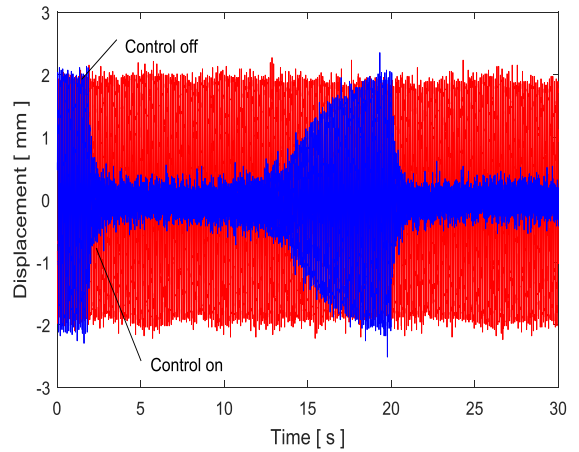


Fig. 17. Experimental results of the repeated controlled and uncontrolled blade vibrations

5. CONCLUSIONS

In this study, vibration of a small-scale wind turbine blade is suppressed using a MR patch layer and electromagnetic actuator under the effect of steady state aerodynamic disturbance. A force based interaction model between MR patch and electromagnet is derived and some characterization works are presented. An LQG controller is designed to attenuate the vibration of the blade structure. Some experiments are realized to show the effectiveness of the proposed MR patch electromagnetic actuator for the transient and steady state aerodynamic loads. The experimental frequency responses and time history responses of the closed loop system demonstrated significant vibration reduction.

References

- [1] G. Yang, Large-Scale magnetorheological fluid damper for vibration mitigation: modeling, testing and control, Ph.D. Dissertation, University of Notre Dame, (2001), <http://cee.uiuc.edu/sstl/gyang2/ch2.pdf>.
- [2] B. F. Spencer, S. Nagarajaiah, State of the art of structural control, *Journal of Structural Engineering*, 129, 845–856, (2003).
- [3] Y. L. Xu, W. L. Qu, and J. M. Ko, Seismic response control of frame structures using magnetorheological/electrorheological dampers, *Earthquake Engineering and Structural Dynamics*, 29, 557-575, (2000).
- [4] R. Stanway, J. L. Sproston, A. K. El Wahed, Applications of electrorheological fluids in vibration control: a survey, *Smart Materials and Structures*, 5, 464-482, (1996).
- [5] K. D. Weiss, J. D. Carlson, D. A. Nixon, Viscoelastic properties of magneto- and electro-rheological fluids, *Journal of Intelligent Material Systems and Structures* 5, 772-775, (1994).
- [6] H. Niu, Y. Zhang, X. Zhang, and S. Xie, Active vibration control of plates using electro-magnetic constrained layer damping, *International Journal of Applied Electromagnetics and Mechanics*, 33(1, 2), 831-837, (2010).
- [7] M. Romaszko, Free vibration control of a cantilever MR fluid based sandwich beam. In *Carpathian*

- Control Conference (ICCC), 2013 14th International (pp. 311-314), May, (2013).
- [8] B. Hu, D. Wang, P. Xia, & Shi, Investigation on the vibration characteristics of a sandwich beam with smart composites-MRF. *World Journal of Modelling and Simulation*, 2(3), 201-206, (2006).
- [9] L. Chen, & C. H. Hansen, Active vibration control of a magnetorheological sandwich beam, *Proc. Acoustics 2005* (Busselton Western Australia), 93-98, (2005).
- [10] A. V. Valevate, Semi-active Vibration control of a beam using embedded magneto-rheological fluids, *Doctoral Dissertation*, Wright State University, (2004).
- [11] V. Rajamohan, R. Sedaghati, and S. Rakheja, Optimal vibration control of beams with total and partial MR-fluid treatments, *Smart Materials and Structures*, 20(11), 115016, (2011).
- [12] C. Hirunyapruk, Vibration control using an adaptive tuned magneto-rheological fluid vibration absorber, *Doctoral Dissertation*, University of Southampton, (2009).
- [13] S. A. Fazelzadeh, M. Azadi, and E. Azadi, Suppression of nonlinear aeroelastic vibration of a wing/store under gust effects using an adaptive-robust controller, *Journal of Vibration and Control*, 23(7), 1206-1217, (2017).
- [14] M. S. Selig, and B. D. McGranahan, Wind tunnel aerodynamic tests of six airfoils for use on small wind turbines. *Journal of Solar Energy Engineering* (Transactions of the ASME), 126(4), 986-1001, (2004).
- [15] D. M. Somers, and M. D. Maughmer, Theoretical aerodynamic analyses of six airfoils for use on small wind turbines, *National Renewable Energy Laboratory (NREL)*, (No. NREL/SR-500-33295), (2003).
- [16] K. Zhou, and J. C. Doyle, *Essentials of robust control upper saddle river*, NJ: Prentice Hall, (104), 88-267, (1998).

Biographies



Fevzi Çakmak Bolat received the B.S and M.S. degree in mechanical engineering from the Atatürk University, Erzurum, Turkey, in 2011. He is currently a research assistant and a Ph.D. student at Gebze Technical University Gebze, Turkey. His research interests are modeling and experimental verification of active vibration control, dynamic system modeling and control, semi-active control of smart materials, and robust control applications.

E-mail: fevzibolat@bayburt.edu.tr



Selim Sivrioğlu received the Ph.D. degree from Chiba University, Chiba, Japan, in 1998. He is currently Professor in the Department of Mechanical Engineering, Gebze Technical University, Gebze, Turkey. His current research interests are smart structures, modeling and experimental verification of superconducting magnetic levitation, active control of magnetic bearings, semi-active control of vehicle suspension systems, robust and adaptive control applications.

E-mail: s.selim@gtu.edu.tr